Comparison of two LES codes for wind turbine wake studies

Sarlak Chivaee, Hamid; Pierella, F.; Mikkelsen, Robert Flemming; Sørensen, Jens Nørkær

Published in:
Journal of Physics: Conference Series (Online)

Link to article, DOI:
10.1088/1742-6596/524/1/012145

Publication date:
2014

Document Version
Publisher's PDF, also known as Version of record

Comparison of two LES codes for wind turbine wake studies

2014 J. Phys.: Conf. Ser. 524 012145

(http://iopscience.iop.org/1742-6596/524/1/012145)

Comparison of two LES codes for wind turbine wake studies

H Sarlak[1], F Pierella[2], R Mikkelsen[1], JN Sørensen[1]

[1] Technical University of Denmark, Lyngby, Denmark.
[2] Norwegian University of Science and Technology, Trondheim, Norway.

E-mail: hsar@dtu.dk

Abstract. For the third time a blind test comparison in Norway 2013, was conducted comparing numerical simulations for the rotor C_p and C_t and wake profiles with the experimental results. As the only large eddy simulation study among participants, results of the Technical University of Denmark (DTU) using their in-house CFD solver, EllipSys3D, proved to be more reliable among the other models for capturing the wake profiles and the turbulence intensities downstream the turbine. It was therefore remarked in the workshop to investigate other LES codes to compare their performance with EllipSys3D. The aim of this paper is to investigate on two CFD solvers, the DTU's in-house code, EllipSys3D and the open-sourse toolbox, OpenFoam, for a set of actuator line based LES computations. Two types of simulations are performed: the wake behind a signle rotor and the wake behind a cluster of three inline rotors. Results are compared in terms of velocity deficit, turbulence kinetic energy and eddy viscosity. It is seen that both codes predict similar near-wake flow structures with the exception of OpenFoam's simulations without the subgrid-scale model. The differences begin to increase with increasing the distance from the upstream rotor. From the single rotor simulations, EllipSys3D is found to predict a slower wake recovery in the case of uniform laminar flow. From the 3-rotor computations, it is seen that the difference between the codes is smaller as the disturbance created by the downstream rotors causes break down of the wake structures and more homogenuous flow structures. It is finally observed that OpenFoam computations are more sensitive to the SGS models.

1. Introduction

LES of wind turbine wakes

Wind turbine wakes and aerodynamics have historically been studied using either analytically-derived empirical models based on experiments [10], or experimental wind tunnel measurements [11]. Wind tunnel measurements suffer from low Reynolds number and scaling issues and analytical models are usually based on questionable simplifying assumptions. With the increase in the computational power and due to the recent wind turbine modeling developments such as introduction of the actuator line modeling technique however, numerical studies have also been recently applied to the simulation of wind turbine wakes and their interactions with the atmospheric boundary layers. LES, in particular, has shown capability of resolving the unsteady nature of the wake flows without the previous concerns [12].

Mikkelsen [13] and Mikkelsen et al. [14] coupled the actuator line, already developed by Sørensen and Shen [15], and actuator disc models with the CFD solver, EllipSys3D. Mikkelsen performed a comprehensive study on the *Tjæreborg* wind turbine and *LM* blade and confirmed

the applicability of the LES for wake studies. Jimenez et al. [23] developed a LES code using dynamic Smagorinsky model and performed wind turbine simulations in the ABL. They used actuator disc representation of the wind turbine using a constant forcing and by comparing with the *Sexbierum* wind farm field data, they showed that LES is capable of investigating the detailed wake flows. Ivanell [16] performed actuator disc simulations of the *Horns Rev* wind farm using a prescribed neutral ABL. They used the rotating AD model implemented by Mikkelsen [13] and investigated the effect of the yaw angle on the wake deficits. This research showed that a better agreement holds between the measurements and the LES computations when the wind direction is not completely aligned with the wind turbines. For the cases with zero yaw degree, however, the wake effects were over-predicted and the downstream turbine power production was correspondingly under-predicted, as compared with the 10-min averaged measurements.

Troldborg et al. [1] conducted a detailed study of the actuator line models in sheared and uniform free-stream and documented the effects of the free stream turbulence as well as other numerical parameters on the wake profiles. The above mentioned simulations [14, 1, 16] were all obtained using a mixed scale SGS model originally proposed by Sagaut [18] and Ta Phuoc [17]. Calaf et al. [2] compared two SGS models on two different CFD codes. The codes used the standard Smagorinsky model and the scale dependent Lagrangian dynamic Smagorinsky model. They simulated a fully developed infinite wind farm and studied the interactions of the wind turbines with the neutrally stratified ABL. The vertical transport of the momentum accross the ABL was investigated using a combination of different rotor arrangements, domain sizes, thrust coefficients and the surface roughness heights and a model for an effective roughness height -representing the turbine effects- were proposed. Porté-Agel et al. [21] performed LES of the wind turbine wakes using both AD and AL approaches. They compared their simulations with the wind tunnel measurements and found that to have the most accurate wake predictions in the region of up to 5 rotors downstream, the rotational effects needs to be included in the wind turbine parametrizations. The wind turbine simulations in the ABL have been mostly performed on the neutral atmospheric stratification. Recently, Lu and Porté-Agel [3] performed LES computations of the wind farms in stably stratified flows using a variant of the dynamic Lagrangian SGS model. Sarlak et al. [7] studied the effects of different SGS models on the actuator line representation of the wind turbine wakes and showed that while different SGS models offer different eddy viscosities, their effects on the turbine performance characteristics is almost negligible. Nevertheless, it is expected that different sub-grid scale models influence the wake delevopment, by shortening the distance at which the tip vortex start to interact with each other and, therefore, the length of the near wake. This paper seeks to investigate effects of both SGS modeling and two different CFD codes on the wake interactions using LES technique.

2. Methodology

In order to compare the computing codes, a set of ordinary turbulent channel flow simulation is performed as an initial test and then the codes are used to compare the performance of different sub-grid scale models when simulating the wake interactions of actuator line-based wind turbine parametrizations. The wake studies are performed using a one-rotor and a three-rotor configuration.

2.1. Numerical solvers

This paper presents a comparison between two well-known CFD solvers in the wind energy community, namely EllipSys3D [4, 5] and the open source wind energy package SOWFA [19]. EllipSys3D is a multi-block structured code solving the incompressible Reylolds average Navier-Stokes (RANS) or LES for various rotor flow configurations. OpenFoam may be configured in a similar manner. Both codes use a collocated grid arrangement and Rhie-Chow type of pressure

velocity coupling, and in this study are run in parallel using Message Passing Interface (MPI) system on the same block structured grids.

The filtered Navier-Stokes equation reads in its vectorized form as

$$\frac{\partial \mathbf{v}}{\partial t} + \mathbf{v} \cdot \nabla \mathbf{v} = -\frac{\nabla p}{\rho} + \nabla \cdot [(\nu + \nu_{sgs}) \nabla \mathbf{v}] + \frac{\mathbf{f}}{\rho}, \quad (1)$$

where ρ and ν are the fluid density and molecular viscosity respectively. $\mathbf{v}$ represents the filtered velocity vector, p is the modified pressure, and $\mathbf{f}$ is the external body force acting on the flow due to the presence of the wind turbine. ν_{sgs} is the eddy viscosity to be specified by the SGS model.

In Ellipsys, the flow was solved by means of a PISO algorithm. A central discretization scheme was used for the convective terms, blended with QUICK in a proportion of $90\% - 10\%$, in order to increase the stability of the solution and avoid numerical wiggles [1] (we will get back to this feature later).

In the OpenFoam implementation the flow was solved by means of a PISO unsteady algorithm with two outer corrector loops. A generalised geometric-algebraic multigrid (GAMG) method was used to solve the pressure equation, with a solver tolerance of 10^{-6}. The momentum equation was solved via a preconditioned bi-conjugate gradient solver, with a convergence tolerance of 10^{-5}.

Components of gradient terms were discretized via Gauss integration coupled with a linear integration of the face values to the cell center. The convective terms of the momentum equation were again discretised via a Gauss integration with linear interpolation. A limited second order accurate linear scheme [8] was used for the discretisation of the divergence terms of the sub-grid scale stress tensor. The diffusion terms were again discretized via Gauss integration with linear interpolation. The same approach was used for the surface normal gradients, with an additional correction in order to take into account for the non-orthogonality of the mesh [20, 9].

2.2. Channel flow simulations

Fully-developed boundary layer flows are of special interest in wind energy and atmospheric sciences for two reasons. First of all, because of the simplicity of the computational domain and the developed flow structures (turbulent production at solid walls and turbulent dissipation), they are useful for code velidations. Secondly, they are used for atmospheric boundary layer (ABL) flow simulations as the flow over very large wind farms with lengths much larger than the height of the ABL, can be considered fully-developed [2].

In order to validate the two computing codes in this paper and examine their sensitivity to the numerical errors, a set of fully developed simulations, in which the flow field is homogeneous both in the streamwise and spanwise directions and the statistics are only dependent upon the distance from the wall, are carried out. A parallel flow between two infinite horizontal plates is simulated. The flow is driven by a constant pressure gradient which balances with the wall shear stress, therefore, after becoming stationary, the flow becomes fully developed and does not accelerate or decelerate in the mean sense any further.

The flow is at $Re_\tau = \frac{hu_\tau}{\nu} = 180$ where u_τ is the friction velocity, ν is the molecular viscosity and h is the channel half-height. Both cases use a grid of 48^3 cells in a domain of $2\pi \times 2 \times 2\pi$ in streamwise (x), vertical (y) and lateral (z) directions, respectively. The grid is uniformly dostributed in the horizontal directions and follows a hyperbolic distribution according to equation 2 for clustering close to the walls,

$$y_j = -\frac{tanh(1 - \frac{2j}{N_y})}{tanh(\gamma)} \quad j = 0, ..., N_y \quad (2)$$

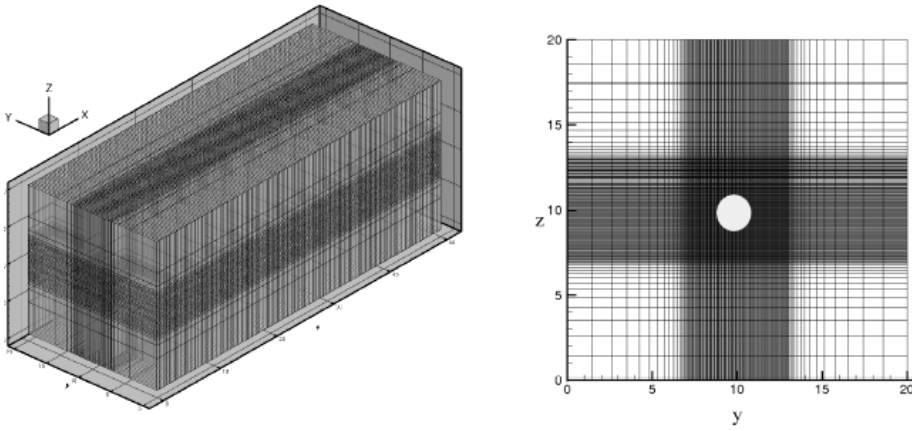

Figure 1. Computational grid used for all actuator line simulations. The hollow circle shows the location and the extent of the turbine model.

with $\gamma = 2.75$, so that the grid height in the first cell close to the wall is $y^+ \sim 1$. The standard Smagorinsky model with $C_s = 0.1$ employing a vanDriest near-wall damping function is used for both codes. See [24] for more details. Both codes are initialized using random velocities and the statistics are obtained after flow stationarity is obtained.

2.3. Wind turbine wake studies

2.3.1. Computational Grids For the simulations of the wind turbine wake a domain of $50R \times 20R \times 20R$ is used in the streamwise (x), spanwise (y) and vertical (z) directions to have a negligible wall blockage effect according to [6]. R represents the rotor radius. The computations are performed on a structured grid with a total of $544 \times 144 \times 144$ cells, both for EllipSys3D and OpenFoam. As from figure 1, the grid is refined in the rotor region and downstream of the rotor throughout the domain, so that the rotor resolution for both EllipSys3D and OpenFoam computations is $j = 20$ grid cells per blade. Outside of the central refined region, 64 cells are positioned (32 for each side), having a strech ratio (size outermost cell over the size of the innermost cell) of 6.

2.3.2. Inflow and boundary conditions For the one and three rotor computations, the simulations are performed in a laminar uniform inflow with a unit reference velocity. The viscosity is set in order to achieve a rotor radius based Reynolds number of $Re_R = 50,000$. Symmetry boundary condition is used for all surrounding walls while inflow and convective outflow BC are reserved for the inlet and outlet planes.

2.3.3. Actuator Line parameters In the actuator line approach, rather than resolving the blade boundary layer with a fine mesh, each blade is modelled as a straight line and the forces are applied to the flow according to the velocity field and the angle of attack. These forces are commonly smeared out by an e.g. Gaussian distribution to the flow field to avoid numerical oscillations [15]. The Gaussian projection width for the current simulations was set to 2.4 the cell size in the equidistant-grid wake region. For the actuator line wake simulations, the *Tjæreborg* turbine is used and the 2D airfoil data were retrieved from [1].

For OpenFoam computations, since the SOWFA actuator line library does not support profile interpolation, the aerodynamic properties of the different airfoils composing the blade were

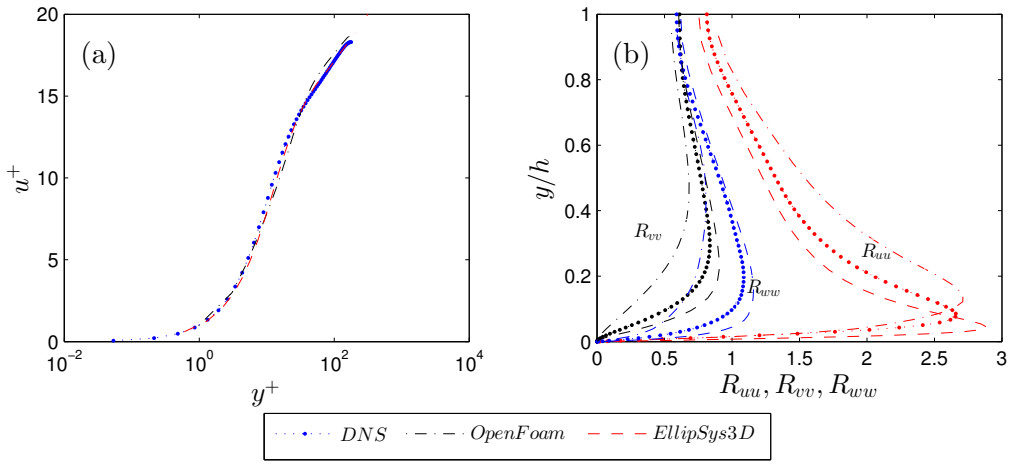

Figure 2. Comparison of Ellipsys3D (dashed lines) and OpenFoam (dot-dashed line) with the DNS [22] (markers) data for the channel flow at $Re_\tau = 180$. (a) Velocity profiles $u^+ = u/u_\tau$. (b) R.M.S. of fluctuations in streamwise (red), vertical (black) and lateral (blue) directions.

interpolated via a MATLAB routine. No Reynolds number interpolation was implemented in the calculations. Glauert's correction factor was used in order to correct for tip losses.

3. Results and discussion

3.1. Channel flow simulations

Figures 2 shows the comparison of Ellipsys3D and OpenFoam for the channel flow. It can be seen that both simulations are able to predict the channel flow with high accuracy especially in terms of the mean, horizontally averaged velocity (figure 2(a)). The R.M.S. values of turbulent fluctuations have also acceptable accuracy as shown in figure 2(b).

3.2. Wake behind the single-rotor and the three-rotor arrangements

In the single rotor simulation, the turbine is located at $7R$ downstream of the inlet. The turbine is spinning at a constant rotational velocity, corresponding to a tip speed ratio of $\lambda = 7.29$. The time step used for the simulation was $dt = 0.005\ s$, chosen in order to limit the space travelled by the blade tip to less than one cell per time step. The relatively small time increment limited the Courant number to a maximum of 0.15 for the whole computational domain and for all the tested set-ups. For every test case, the computation was run for 75 s to allow the wake to fully develop and to reach the outlet of the computational domain, after which the flow quantities were then sampled for other 125 s. The sampling time proved to be sufficient for the fluctuating quantities to stabilize.

The wake of a single turbine in laminar flow is shown in figure 3. The instantaneous velocities show a different trend for the two codes. While the predicted velocity deficit right behind the rotor is comparable, OpenFoam predicts a much faster destabilization of the wake structure already at $x/R \sim 15$ from the rotor. The simulations from EllipSys3D predict a stable vortex system which does not break down until very far downstream $x/R \sim 35$. The resolved turbulent streamwise Reynolds stress indicates a distinct pattern for the OpenFoam simulation with its maximum values at around $x/R = 25$. On the other hand, EllipSys3D predicts a virtually

zero velocity fluctuation until $x/R = 30$, after which the wake starts to become unstable. This means that in the EllipSys3D simulation, the tip vortices form a uniform vortex sheet, inducing no velocity oscillations. On the other hand, OpenFoam predicts a less uniform vortex sheet which interact much closer to the rotor. This is probably due to a slightly inconsistent 2D airfoil interpolation or by a marginally lower tip speed ratio. The contour plot of the eddy viscosity also confirms that in the EllipSys3D case, the vorticity is shed only at the blade tip and root, however, in the OpenFoam computations, the vorticity shedding pattern is not as homogeneous. Despite imposing a zero eddy viscosity at the inlet, non-zero values are present at very short downstream distances from the inlet. This behavior is considered to be somewhat unphysical, since, in that region, the mean flow shear is not strong to produce such high eddy viscosities. This could be a further reason explaining the early destabilization of the vortex structures obtained by OpenFoam computations.

In order to compare the results of the turbulent wake one can introduce synthetic turbulence. In this test case, the effect of the turbulence is rather studied by positioning a wind turbine in the wake of two upstream machines, deemed to be more relevant for industrial applications. The turbines are placed at $x/R = 7, 13, 19$ from the inlet in an in-line configuration and then the statistics are compared for different locations downstream of the first rotor. Both codes are run using the standard Smagorinsky model. Figure 4 shows the visual comparison of the instantaneous velocity, turbulence intensity, and the normalized eddy viscosities. Here the second turbine causes the wake of the upstream turbine to break-up earlier as compared with the signle rotor arrangement. All the three turbines are operating at the same tip speed ratio of $\lambda = 7$: by the analysis of the mean velocity plots (figure 4a) it is possible to see how the second turbines efficiently extracts energy only in the tip region, while the root is probably stalled and extracts no energy from the flow. This would bring a large amount of vorticity shedding into the wake and that additional turbulent kinetic energy is created in the inner shear induced by the presence of the second turbine. The resolved streamwise Reynolds stresses exhibit very similar patterns, while the sub-grid scale viscosity predicted by the OpenFoam implementation of the Smagorinsky model is still singificantly lower than the corresponding EllipSys3D case. Again, unphysical non-zero sub-grid viscosity is observed in the OpenFoam simulation upstream from the turbine.

Figure 5 shows a quantitative comparison of the mean streamwise velocity, as well as normal and shear components of the stress tensor at four locations, $x/R = 0, 10, 20, 30$ behind the turbine for the signle rotor arrangement. Comparison is made using the no SGS model (NO), Smagorinsky model (SM) and the standard dynamic Smagorinsky model (DS). Close to the rotor, where the flow is mostly laminar, the models perform quite similarly and predict a near-wake mean velocity profile. At $20R$ from the rotor, the EllipSys3D simulations maintain a very high velocity deficit and show a very close agreement amongst all the models. OpenFoam simulations start to deviate the EllipSys3D counterpart already at $x/R = 10$ and the differences begin to grow as we go further downstream. At $x/R = 30$, all of the OpenFoam cases, except the NO model, exhibit a Gaussian wake profile unlike EllipSys3D cases. The differences are more pronounced in the TKE plots. Close to the rotor, the NO model OpenFoam case overpredicts the TKE significantly, whereas all other cases predict very similar values. Again, the differences begin to dominate with increasing the distance from the upwind rotor. The results also show that, for the OF simulation, the usage of a blend of upwind and central differencing for the convective term does not significantly alter the mean velocity profiles. As for the resolved TKE, it generates smoother average curves indicating a better statistical convergence.

As for the three-rotors arrangement, figure 6 shows the quantitative comparison of the mean streamwise velocity, as well as normal and shear components of the stress tensor at four locations downstream of the first upstream turbine. Here, the mean velocity deficit induced by the turbines are very similar, although the OpenFoam NO model tends to deviate from the rest of the cases.

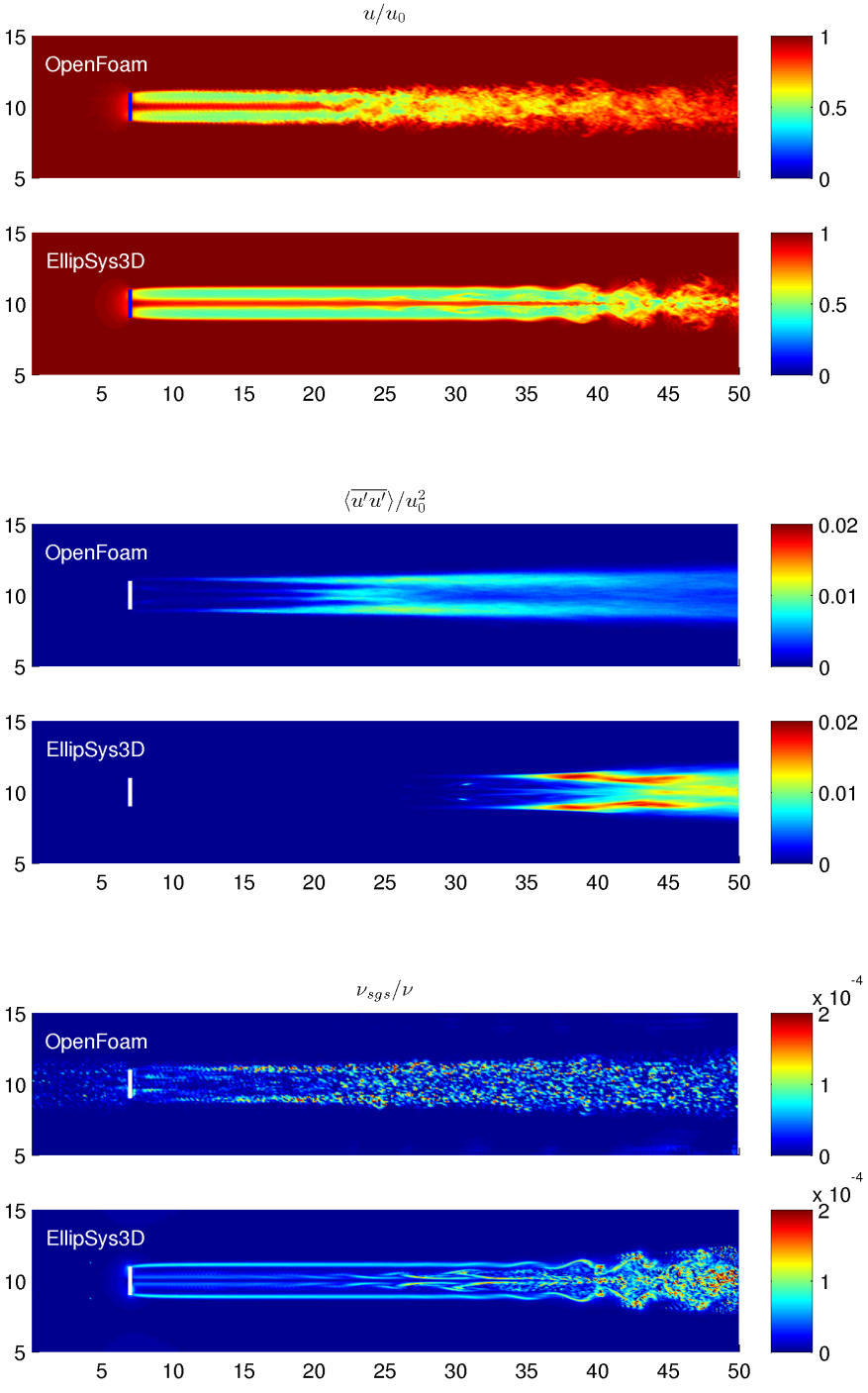

Figure 3. Comparison of Ellipsys3D and OpenFoam for the wake of a single turbine in laminar flow, with a Dynamic Smagorinsky sub-grid scale model. (a) streamwise velocity, (b) $\langle\overline{u'u'}\rangle/U_o^2$, (c) Eddy viscosity ratio.

The analysis of the shear stress, which determines the momentum transfer from the free stream and into the wake, as well as the resolved TKE show that the values predicted by both codes are similar, again with the exception of the OpenFoam's NO model, which overpredicts the values in the near wake but recovers with the rest of the cases in the far wake. The resolved TKE shows the largest differences among the rest of the cases, especially at $x/R = 20$, where the value predicted by *EllipSys3D SM* model is almost twice as large as the *OpenFoam DS* case.

4. Conclusions

In this paper, the wind turbine wake interactions were investigated and a comparison was performed between two well-known CFD codes, EllipSys3D and OpenFoam. From the comparison, it can be concluded that generally, results of EllipSys3D and OpenFoam for the near-wake are in agreement especially when a SGS model is used in OpenFoam. This is particularly the case when comparing the mean velocity profiles. For the signle rotor simulations in the laminar free-stream, the tip vortices simulated by OpenFoam break down much faster than EllipSys3D. It was also seen that the results for the 3-rotor arragement are in better agreement as compared with the signle rotor case since the former is less sensitive to small disturbances that might trigger instabilities etc.

References

[1] Troldborg N, Sørensen JN and Mikkelsen RF 2010 Numerical simulations of wake characteristics of a wind turbine in uniform inflow *J Wind Energy* (**13**)1 86-99.
[2] Calaf, M., Meneveau, C., and Meyers, J. 2010 Large eddy simulation study of fully developed wind-turbine array boundary layers. *Physics of Fluids*, **22**(015110).
[3] Lu H., and Porte-Agel, F. 2011 Large-eddy simulation of a very large wind farm in a stable atmospheric boundary layer *Physics of Fluids*, **23**, 065101.
[4] Michelsen JA 1992 *Basis3D- A platform for development of multiblock PDE solvers*, Technical report AFM 92-05, Technical University of Denmark.
[5] Sørensen NN 1995 *General purpose flow solver applied to flow over hills*, Risø-R-827-(EN), RisøNational Laboratory, Denmark.
[6] Baetke F and Werner H 1990 Numerical simulation of turbulent flow over surface-mounted obstacles with sharp edges and corners *J Wind Eng Ind Aerod* **(35)** 129-47.
[7] Sarlak H., Meneveau C., Sørensen JN, and Mikkelsen R. 2014 Quantifying the impact of subgrid scale models in actuator-line based LES of wind turbine wakes in laminar and turbulent inflow, Direct and Large-Eddy Simulation IX ERCOFTAC Series, Springer (accepted).
[8] Sweby PK 1984 High resolution schemes using flux limiters for hyperbolic conservation laws. *SIAM journal on numerical analysis*, 21(**5**):995–1011.
[9] Jasak H 1996 *Error analysis and estimation for the finite volume method with applications to fluid flows*. PhD thesis, Imperial College London.
[10] Frandsen S et al. 2006 Analytical modelling of wind speed deficit in large offshore wind farms. *Wind energy* **9**.1-2 pp. 39-53.
[11] Bartl J Pierella F, and Saetrana L 2012 Wake measurements behind an array of two model wind turbines. *Energy Procedia* 24 pp. 305-312.
[12] Sørensen, JN 2011 Aerodynamic aspects of wind energy conversion *Ann. Rev. Fluid Mech.* **43** pp. 427-448.
[13] Mikkelsen R 2003 Actuator disc methods applied to wind turbines. PhD thesis, Tech. Univ. of Denmark.
[14] Mikkelsen R et al. 2007 Analysis of power enhancement for a row of wind turbines using the actuator line technique *J Phys.: Conf. Ser.*. **75**. No. 1..
[15] Sørensen JN, and Shen WZ 2002 Numerical modeling of wind turbine wakes *Journal of fluids engineering* 124.2 pp. 393-399.
[16] Ivanell S et al. 2009 Analysis of numerically generated wake structures *Wind Energy* **12**.1 pp. 63-80.
[17] Ta Phuoc L 2004 Modeles de sous-maille appliques aux ecoulements instationnaires et decolles *Journee Thematique DRET, Paris*.
[18] Sagaut P 1995 Simulations num eriques d ecoulements lecoll les avec des mod'eles de sous-maille. PhD thesis, Univ. Pierre et Marie Curie.
[19] Churchfield M and Lee S Ntwc - simulator for offshore wind farm applications (sowfa). Website, December 2012. http://wind.nrel.gov/designcodes/simulators/sowfa/.
[20] OpenCFD. *Openfoam user guide OpenFOAM Foundation*, 2(1), 2011.

[21] Porté-Agel F et al. 2011 Large-eddy simulation of atmospheric boundary layer flow through wind turbines and wind farms *J. Wind Eng. Ind. Aerodyn.* **99**.4 pp. 154-168.
[22] Moser RD, Kim J and Mansour NN 1999 Direct numerical simulation of turbulent channel flow up to Re= 590 *Phys. Fluids* **11**.4 pp. 943-945.
[23] Jimenez A, Crespo A, Migoya, E and García, J. 2007 Advances in large-eddy simulation of a wind turbine wake *J. Phys.:Conf. Ser.* **75** pp. 12-41.
[24] Sarlak H 2014 *Large Eddy Simulation of Turbulent Flows in Wind Energy*, PhD Thesis (submitted), Tech. Univ. Denmark.

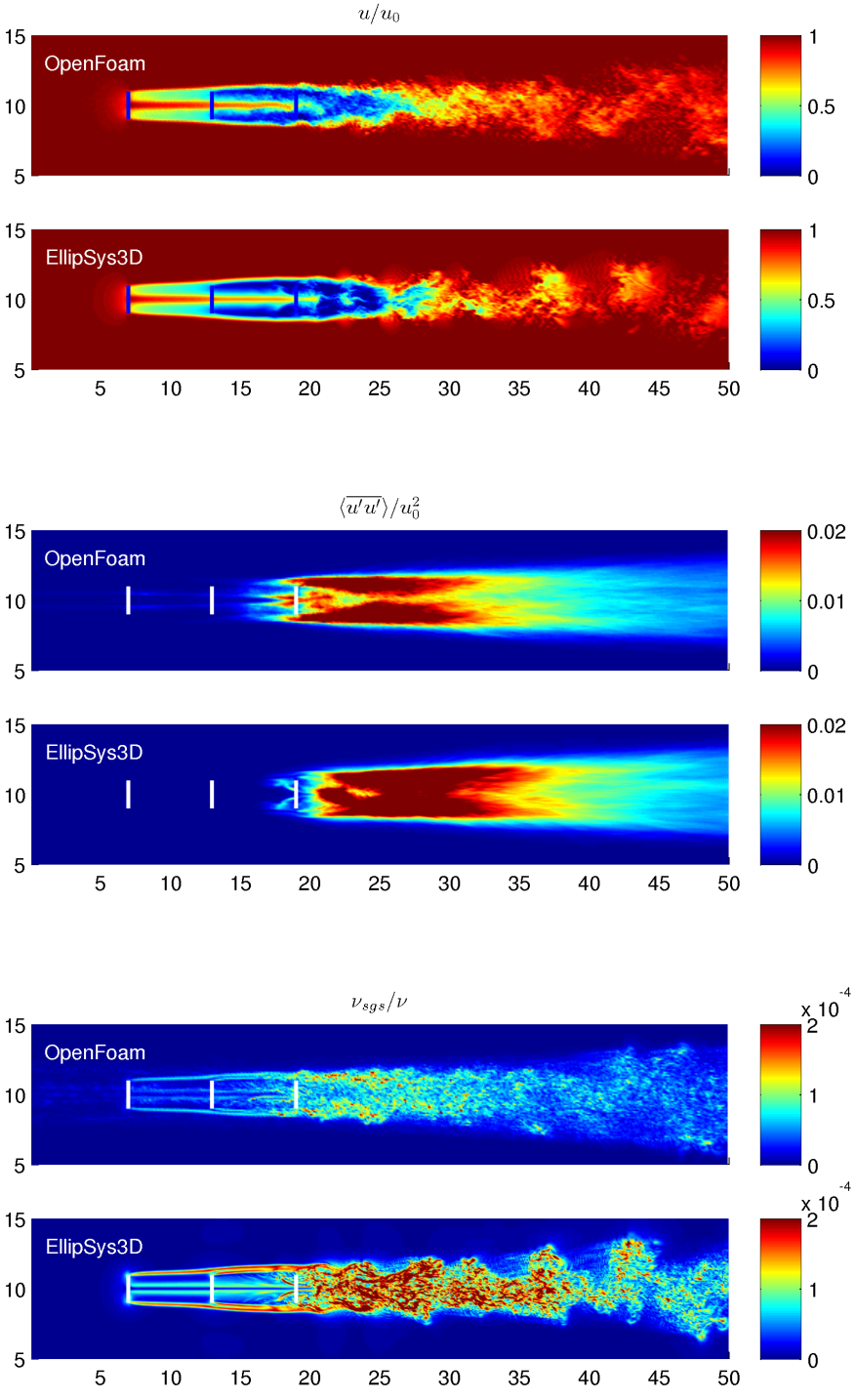

Figure 4. Comparison of EllipSys3D and OpenFoam for the wake of three aligned turbines in laminar flow, using a Smagorinsky sub-grid scale model. (a) streamwise velocity, (b) $\langle \overline{u'u'} \rangle / U_o^2$, (c) Eddy viscosity ratio.

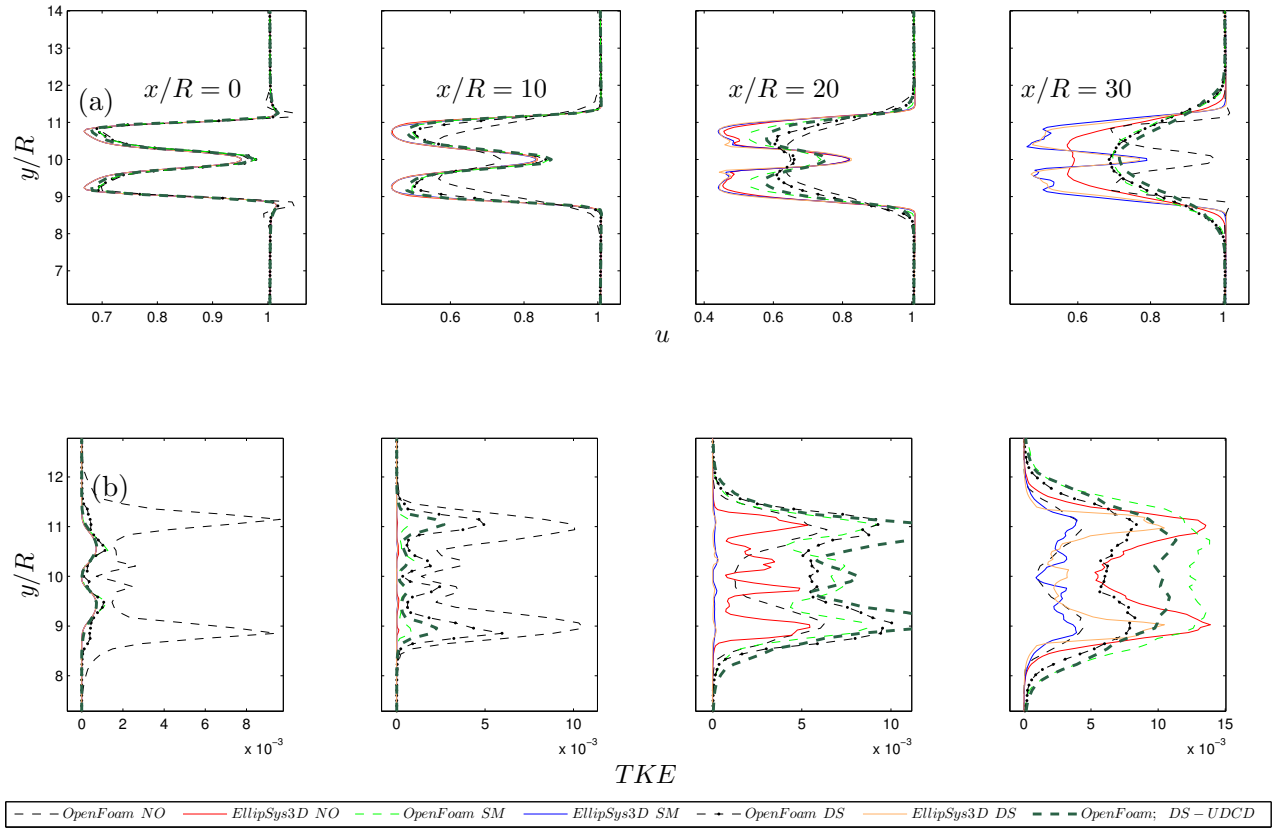

Figure 5. Plots of (a) mean streamwise velocity $\langle\overline{u}\rangle$, and (b) resolved TKE at different locations downstream of the turbine in the 1-rotor arrangement. NO: no SGS model; SM: Smagorinsky model; DS: dynamic Smagorinsky model. The *OpenFoam DS-UDCD* refers to OpenFoam computations performed by a blend of central and upwind discretization schemes. As can be seen, no general conclusion can be drawn regarding the effect of blending in the OpenFoam simulations.

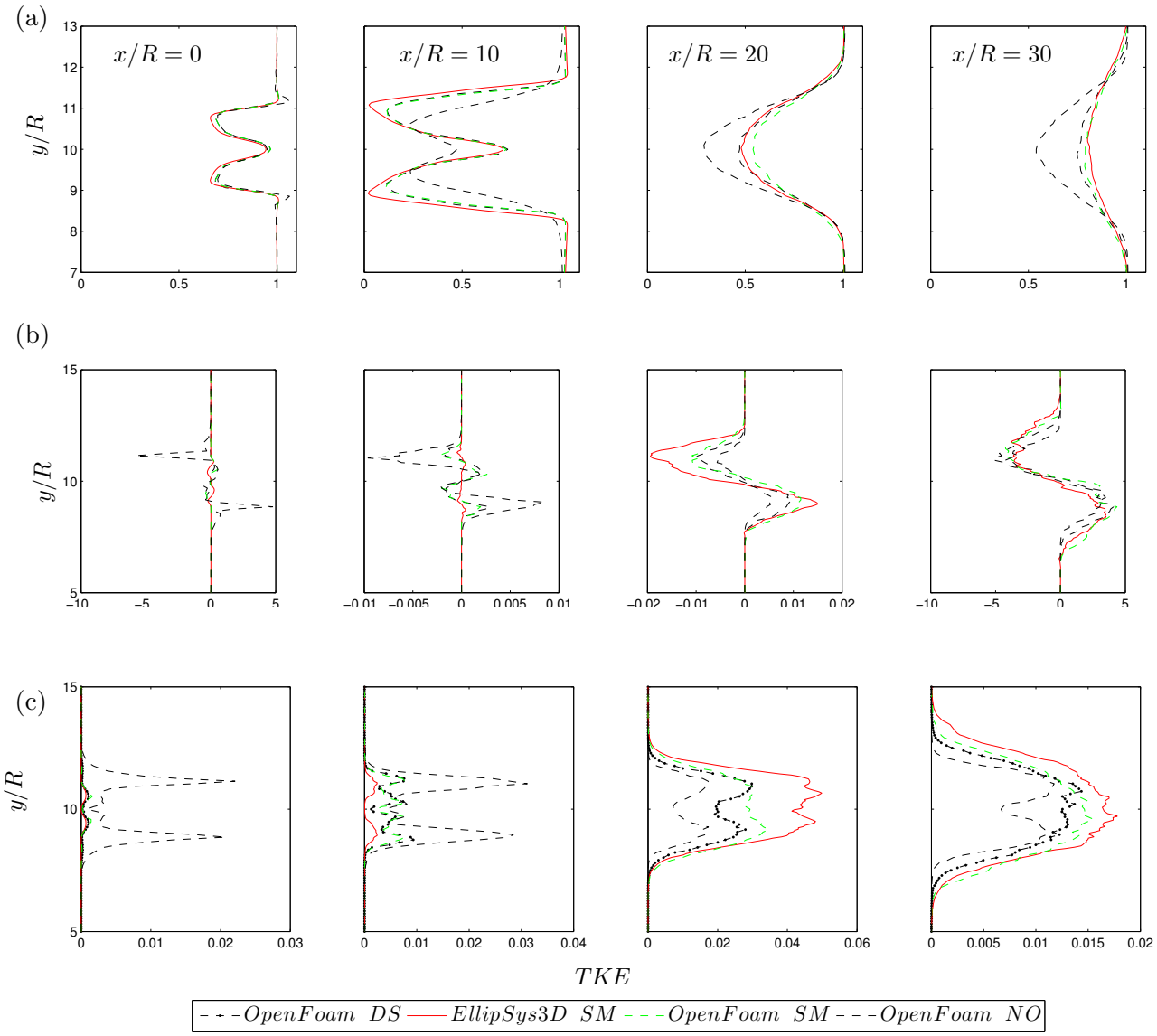

Figure 6. Plots of (a) mean streamwise velocity $\langle \overline{u} \rangle$, (b) shear stress $\langle \overline{u'v'} \rangle / U_o^2$, and (c) TKE at different locations downstream of the first turbine in the 3-rotor arrangement.